Magnetoconductance of carbon nanotube p-n junctions

A. V. Andreev
Department of Physics, University of Washington, Seattle, Washington 98195-1560, USA
(Dated: June 5, 2007)

The magnetoconductance of p-n junctions formed in clean single wall carbon nanotubes is studied in the noninteracting electron approximation and perturbatively in electron-electron interaction, in the geometry where a magnetic field is along the tube axis. For long junctions the low temperature magnetoconductance is anomalously large: the relative change in the conductance becomes of order unity even when the flux through the tube is much smaller than the flux quantum. The magnetoconductance is negative for metallic tubes. For semiconducting and small gap tubes the magnetoconductance is nonmonotonic; positive at small and negative at large fields.

PACS numbers: 75.47.Jn, 73.23.Ad, 73.63.Fg

Magnetoconductance arises from the orbital and Zeeman coupling of electrons to the external magnetic field, H. As long as the flux through the crystalline unit cell is much smaller than the flux quantum $\Phi_0 = hc/e$ magnetotransport may be described in the semiclassical approximation [1] ignoring the band structure changes due to the presence of H. In most crystals this condition holds at all experimentally realizable fields. Recently much attention was focused on magnetotransport properties of carbon nanotube devices. Because of their large radius the magnetic field affects the one-dimensional electron spectrum [2] even at relatively weak fields. This leads to interesting magnetotransport phenomena [3, 4, 5, 6, 7, 8, 9, 10].

In this paper we show that the magnetic field dependence of the one-dimensional band structure results in a peculiar mechanism of magnetoconductance of p-n junctions in carbon nanotubes. This mechanism is relevant to the magnetoresistance of nominally undoped metallic and small gap nanotubes placed on an insulating substrate. In this case the long range disorder potential caused by charged impurities in the substrate creates p- and n- regions in the tube, and backscattering of electrons arises mainly from the gaps between p- and n- regions, where the semiclassical description of electron transport fails.

We study the magnetoconductance of a p-n junction formed in a clean single wall carbon nanotube for magnetic fields parallel to the tube axis. The device is depicted in Fig. 1 *a*). The p- and n- regions can be formed by appropriately biasing the top gates. Such devices were recently used to measure [11] thermodynamic properties of electron liquid in carbon nanotubes. It is shown below that for realistic device parameters similar to those of Ref. 11 the low temperature magnetoconductance becomes of order unity while the flux Φ through the tube cross-section is much smaller than Φ_0.

Before proceeding to detailed calculations let us qualitatively discuss the origin of strong magnetoconductance. We choose the x- and y- axes to be respectively along the tube axis and along its circumference. The one-dimensional electron sub-band spectrum is determined by intersections of the graphene Brillouin zone with the $k_y = (\Phi/\Phi_0 + m)/R$ lines, see the inset in Fig. 1 *b*). Here R is the tube radius and m an integer. The electron spectrum near the K and K' points becomes $\pm\sqrt{\Delta^2 + (\hbar v p_x)^2}$, where $v \approx 8 \times 10^5\, m/s$ is the electron velocity in graphene, and Δ is half the energy gap between the valence and conduction sub-bands. In the center region between the p- and n- banks the external potential is assumed to be approximately linear, $U(x) = eEx$, where e is the electron charge and E the electric field. The tilting of electron energy bands in the external potential produces a spatial region of width $2x_0 = 2\Delta/eE$, where electron motion is classically forbidden, see Fig. 1 *b*). The device conductance is governed by the Landau-Zener tunneling across this region. With exponential accuracy the tunneling probability may be

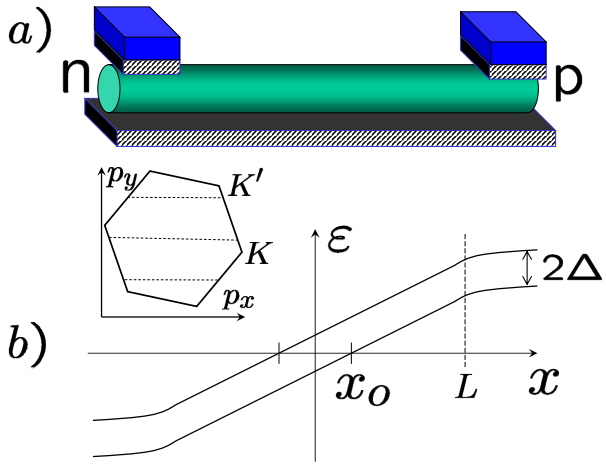

FIG. 1: a) Device sketch: a nanotube rests on an insulating substrate. The n- and p- regions are created by biasing the top gates. b) Band diagram of the device. Tilted solid lines represent the bottom of the conduction and the top of the valence bands. The width of the center region is $2L$. The width of the classically forbidden region is $2x_o = 2\Delta/eE$. Inset: one dimensional spectrum is obtained by dissecting the graphene Brillouin zone by the $p_y = 0$ line (dashed line). The low energy states lie in the vicinity of K and K' points.

found in the WKB approximation. The electron momentum p_x along the tube depends on the position as $p_x = \sqrt{(eEx-\epsilon)^2-\Delta^2}/v$. This gives the transmission probability $\mathcal{T} = \exp\left(\frac{2}{\hbar}\mathrm{Im}\int p_x dx\right) = \exp[-\pi\Delta^2/(\hbar veE)]$. The rigorous calculation given below shows that the pre-exponential factor is equal to unity. The magnetoconductance arises from the flux dependence of the band gap [2], $\Delta = \Delta_0 \pm \hbar v\Phi/R\Phi_0$, where Δ_0 is half-the band gap at zero flux and the $\pm$ sign corresponds to the different valleys, K and K'. Accounting for electron spin and the two valleys and neglecting the Zeeman splitting one obtains for the device conductance

$$G_0 = \frac{2e^2}{h}\sum_{j=1,2}\exp\left[-\frac{\pi\hbar v}{eER^2}\left(\frac{\Delta_0 R}{\hbar v}+\frac{(-1)^j\Phi}{\Phi_0}\right)^2\right]. \tag{1}$$

If the electric field is not too strong, $eER \ll \hbar v/R$, the magnetoconductance becomes of order unity while the flux is still small, $\Phi \ll \Phi_0$. In the case of metallic tubes, $\Delta_0 = 0$, the magnetoconductance is negative. For semiconducting and small gap tubes the magnetoconductance is nonmonotonic; positive at small fields and negative at large ones. The conductance maximum is attained at $\Phi_{max} \approx \Phi_0\Delta_0 R/\hbar v$. For semiconducting tubes, $\Delta_0 \approx \hbar v/3R$, this gives $\Phi_{max} \approx \Phi_0/3$. For small gap tubes the zero flux gap arises only due to curvature effects and is rather small, $\Delta_0 \ll \hbar v/R$. In this case the conductance maximum is achieved at $\Phi_{max} \ll \Phi_0$. A nonmonotonic magnetoresistance was recently observed in Ref. 8 in nanotube devices with a different geometry.

In the noninteracting electron approximation the magnetoconductance only weakly depends on the temperature T as long as the latter is smaller than the Fermi energy in the banks. In this regime the energies of electrons participating in transport lie in the narrow band of width T around the chemical potential. In this energy range deviations of electric potential from the linear form $U(x) \approx eEx$ are negligible. This results in energy-independent transmission coefficient and thus temperature-independent conductance.

In the presence of electron-electron and electron-phonon interactions electrons can be transferred between the p- and n- regions at finite temperature by thermal activation. At $T \gg |\Delta - \Delta_0| = \hbar v\Phi/R\Phi_0$ the rate of inelastic processes is practically independent of the magnetic field and magnetoconductance arises mainly from the tunneling mechanism discussed above. In this regime inelastic transfers shunt the tunneling mechanism and suppress magnetoconductance. A crude estimate of the characteristic temperature T^*, above which the magnetoconductance suppression becomes significant, can be obtained in the tunneling regime by equating the activation rate, $\sim \int_0^\infty \frac{dx}{\ell_{in}}\exp[-(\Delta+eEx)/T] = \frac{T}{eE\ell_{in}}\exp(-\Delta/T)$, with ℓ_{in} being the inelastic mean free path, to the tunneling rate, $\sim \exp\left(-\frac{\pi\Delta^2}{eE\hbar v}\right)$. According to this estimate the noninteracting electron result, Eq. (1) provides a good description of the conductance for $T < eER$.

At zero temperature the finite reflection amplitude at the p-n contact leads to the appearance of Friedel oscillations in the electron density. The additional scattering of electrons from the Friedel oscillations in the presence of electron-electron interactions gives a correction [12] to the noninteracting result for the device conductance, Eq. (1). This correction is evaluated below to first order in electron-electron interaction. It is given by Eq. (15) and is plotted in Fig. 2 b). It remains small even if the interaction constant, $e^2/\hbar v$ is of order unity.

The device conductance in the noninteracting electron approximation, Eq. (1), immediately follows from the results of Cheianov and Falko [13] for a graphene p-n junction that were obtained using transfer matrices. Below we present a consideration in terms of wave functions that is more convenient for the treatment of the interaction correction to magnetoconductance. Electron eigenstates of energy ε obey the Dirac equation, which by an appropriate basis choice can be cast in the form

$$[U(x) - \varepsilon - i\hbar v\sigma_z\partial_x + \Delta\sigma_y]\psi = 0,$$

where σ_i are Pauli matrices. Introducing the dimensionless coordinate $\xi = eEx/\sqrt{eE\hbar v}$, energy $\epsilon = \varepsilon/\sqrt{eE\hbar v}$, and momenta $q = \Delta/\sqrt{v\hbar eE}$ and $k(\xi) = (U(\xi) - \varepsilon)/\sqrt{v\hbar eE}$ we rewrite this equation as

$$\begin{pmatrix} k(\xi)-i\partial_\xi & -iq \\ iq & k(\xi)+i\partial_\xi \end{pmatrix}\begin{pmatrix} u \\ v \end{pmatrix} = 0. \tag{2}$$

The dimensionless momentum $k(\xi)$ changes from $-k_f$ at $\xi \to -\infty$ to $+k_f$ at $\xi \to +\infty$, where $k_f \gg 1$ is the dimensionless Fermi momentum in the banks. In the center region between the banks the coordinate-dependent momentum $k(\xi)$ is linear in ξ, $k(\xi) \approx \xi - \epsilon$, and the spinor amplitudes u and v satisfy the differential equation,

$$(\partial_z^2 + a + z^2)f = 0.$$

Here $a = i - q^2$ for u, and $a = -i - q^2$ for v, and we introduced the difference coordinate, $z = \xi - \epsilon$. The independent solutions of this equation are parabolic cylinder functions [14] that can be expressed in terms of the confluent hypergeometric function $F(\alpha,\gamma,z)$,

$$f_e(z) = \exp\left(-i\frac{z^2}{2}\right)F\left(\frac{1}{4}+\frac{ia}{4},\frac{1}{2},iz^2\right),$$
$$f_o(z) = z\exp\left(-i\frac{z^2}{2}\right)F\left(\frac{3}{4}+\frac{ia}{4},\frac{3}{2},iz^2\right).$$

Two linearly independent solutions of Eq. (2) are

$$\psi_1 = e^{-\frac{\pi q^2}{4}}\begin{pmatrix} u_e \\ -u_o^* \end{pmatrix}, \quad \psi_2 = e^{-\frac{\pi q^2}{4}}\begin{pmatrix} -u_o \\ u_e^* \end{pmatrix}, \tag{4}$$

where

$$u_e(z) = \exp\left(-i\frac{z^2}{2}\right) F\left(-i\frac{q^2}{4}, \frac{1}{2}, iz^2\right), \quad (5a)$$

$$u_o(z) = q\, z \exp\left(-i\frac{z^2}{2}\right) F\left(\frac{1}{2} - i\frac{q^2}{4}, \frac{3}{2}, iz^2\right). \quad (5b)$$

Equation (2) conserves the current along the tube axis, $I_x = \psi^\dagger \sigma_z \psi$. From the form of the current operator it is clear that the top/bottom components of the pseudospinor ψ represent the amplitudes of the right-/left- moving waves. Thus the scattering states incident from the left, ψ_L, and right, ψ_R, can be found by requiring that the bottom/top component of the spinor vanish at $\xi \to \pm\infty$. Using Eqs. (4) and (5) and the large distance asymptotics of the confluent hypergeometric function [14],

$$F(\alpha, \gamma, z \to \infty) \approx \frac{\Gamma(\gamma)}{\Gamma(\gamma - \alpha)}(-z)^{-\alpha} + \frac{\Gamma(\gamma)}{\Gamma(\alpha)} e^z z^{\alpha - \gamma}, \quad (6)$$

we obtain for the scattering states incident from the right and left,

$$\psi_L = \begin{pmatrix} u_L \\ v_L \end{pmatrix} = \frac{\psi_1 + \alpha\, \psi_2}{\sqrt{1 + |\alpha|^2}}, \quad (7a)$$

$$\psi_R = \begin{pmatrix} u_R \\ v_R \end{pmatrix} = \frac{\psi_2 - \alpha^*\, \psi_1}{\sqrt{1 + |\alpha|^2}}. \quad (7b)$$

Here α is given by

$$\alpha = e^{-i\frac{\pi}{4}} \frac{q}{2} \frac{\Gamma\left(\frac{1}{2} - i\frac{q^2}{4}\right)}{\Gamma\left(1 - i\frac{q^2}{4}\right)}, \quad |\alpha|^2 = \tanh\frac{\pi q^2}{4}. \quad (8)$$

The $z \to \pm\infty$ asymptotics of the right-moving wave (the top spinor component) in the scattering states ψ_L and ψ_R are;

$$u_L(z) \approx \frac{\sqrt{\pi} e^{-\frac{\pi q^2}{8}} [1 - \mathrm{sgn}(z)|\alpha|^2]\, |z|^{i\frac{q^2}{2}} e^{-i\frac{z^2}{2}}}{\sqrt{1 + |\alpha|^2}\Gamma\left(\frac{1}{2} + i\frac{q^2}{4}\right)}, \quad (9a)$$

$$u_R(z) \approx -\frac{q}{2} \frac{\sqrt{i\pi} e^{-\frac{\pi q^2}{8}} [1 + \mathrm{sgn}(z)]\, |z|^{i\frac{q^2}{2}} e^{-i\frac{z^2}{2}}}{\sqrt{1 + |\alpha|^2}\Gamma\left(1 + i\frac{q^2}{4}\right)}. \quad (9b)$$

From Eq. (9a) one finds the transmission amplitude,

$$t_0 \equiv \lim_{\xi \to +\infty} \frac{u_L(\xi)}{u_L(-\xi)} = \frac{1 - |\alpha|^2}{1 + |\alpha|^2} = \exp\left(-\frac{\pi q^2}{2}\right).$$

This gives the transmission coefficient is $\mathcal{T}_0 = \exp(-\pi q^2)$, in agreement with Ref. 13. Expressing q in terms of the system parameters using expressions presented in the text above Eq.(2), and taking into account the magnetic field dependence of the energy gap one obtains the device conductance, Eq. (1).

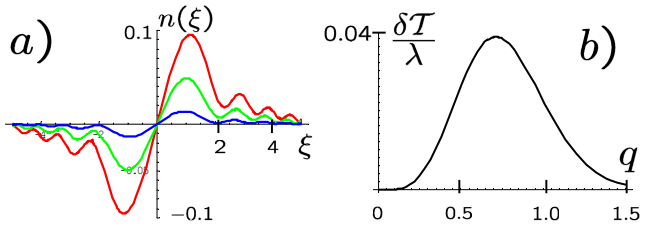

FIG. 2: a) Dimensionless electron density as a function of ξ for $q = 0.3$, $q = 0.6$, and $q = 0.9$. b) The ratio of the correction to the transmission coefficient to the interaction constant λ, Eq. (15), as a function of q.

Next we evaluate the first interaction correction to Eq. (1) at zero temperature. To first order in interaction the correction to the device conductance can be obtained by considering the change in the transmission amplitude for a particle at the Fermi level that arises from the additional scattering from the Hartree-Fock potential induced by the electron density [12]. The induced Hartree-Fock potential has two qualitatively different effects on the transmission amplitude: i) By enhancing the effective electric field inside the classically forbidden region it increases the tunneling amplitude, and ii) It causes additional backscattering from the Friedel oscillations in the classically allowed region. The analysis below shows that repulsive interaction increases the transmission amplitude.

Using Eqs. (5) and (6) it is easy to show that the spinor wave functions in Eq. (4) are normalized to a δ-function of the dimensionless energy,

$$\int_{-\infty}^{\infty} d\xi \psi_i^\dagger(\xi - \epsilon)\psi_j(\xi - \epsilon') = 2\pi\delta(\epsilon - \epsilon')\delta_{ij}. \quad (10)$$

Therefore the electron density, upon subtraction of the uniform ion background, is

$$n(\xi) = \sum_{i=1,2} \int_{-\infty}^{\infty} \frac{\mathrm{sign}(-\epsilon) d\epsilon}{4\pi} \psi_i^\dagger(\xi - \epsilon)\psi_i(\xi - \epsilon). \quad (11)$$

In this equation the energy is measured from the Fermi level and the electron hole symmetry of the problem was used. Plots of electron density, Eq. (11), for different values of q are presented in Fig. 2 a). The Friedel oscillations in charge density appear only at finite refection amplitude and fall off as $1/\xi^2$. The extra power of $1/\xi$ in comparison with the usual one-dimensional Fermi gas arises from the linearly growing external potential. Because of the fast decay of the oscillations the correction to the transmission amplitude is free from infrared divergences and arises from distances $x \sim \sqrt{\hbar v/eE}$.

Below we consider the case of a short range interaction. This should be a reasonable approximation because the Fourier transform of the Coulomb interaction depends on the transferred momentum only logarithmically. Since the characteristic scattering momentum is $\sqrt{\hbar e E/v}$ the

dimensionless interaction constant can be estimated as $\lambda \sim \frac{1}{1+\kappa}\frac{e^2}{\hbar v}\ln\frac{eER^2}{\hbar v}$, where κ is the dielectric constant of the substrate. We restrict the consideration to metallic tubes, for which electron spectra in the presence of the flux remain degenerate in the two valleys. Then the Hartree-Fock potential is $V(\xi) = 3\lambda\, n(\xi)$, where the factor $3 = 4 - 1$ arises from the spin and valley degeneracy.

In the presence of the perturbation potential the wave incident from the left at the Fermi level, $\epsilon = 0$, can be written as $\psi_L(\xi) + \chi(\xi)$. The correction, $\chi(\xi)$, to the wave function satisfies the equation $[\hat{H}_0 + V(\xi)]\chi(\xi) = -V(\xi)\psi_L(\xi)$ with $\hat{H}_0 = \xi - i\partial_\xi\sigma_z + q\sigma_y$ being the unperturbed Hamiltonian. To first order in perturbation the solution of this equation is

$$\chi(\xi) = \int d\xi' G^R(\xi,\xi')V(\xi')\psi_L(\xi'), \qquad (12)$$

where $G^R(\xi,\xi') = (\hat{H}_0 + i\eta)^{-1}$ is the Green's function that can be expressed in terms of the spinors in Eq. (4),

$$G^R(\xi,\xi') = \sum_{i=1,2}\int_{-\infty}^{\infty}\frac{d\epsilon}{2\pi}\frac{\psi_i(\xi-\epsilon)\psi_i^\dagger(\xi'-\epsilon)}{\epsilon + i\eta}. \qquad (13)$$

In order to find the correction to the transmission amplitude one needs only the large distance asymptotics of $\chi(\xi)$. Therefore only the on-shell part of the Green's function will contribute to Eq. (12) at $\xi \to \infty$,

$$\chi(\xi) = -\frac{i}{2}\sum_i \psi_i(\xi)\int d\xi'\psi_i^\dagger(\xi')V(\xi')\psi_L(\xi'). \qquad (14)$$

Since the wave functions $\psi_{1,2}$ are related to the scattering states $\psi_{L,R}$ by the unitary transformation Eq. (7) the sum over i in Eq. (14) can be understood to run over $i = L, R$. Next we notice that for $i = L$ the integral in Eq. (14) is purely real. Therefore this term will only change the phase of the transmission amplitude, but not its modulus. Thus to compute the first correction to the transmission amplitude we may replace $\chi(\xi)$ by

$$\tilde{\chi}(\xi) = -\frac{i}{2}\psi_R(\xi)\int d\xi'\psi_R^\dagger(\xi')V(\xi')\psi_L(\xi').$$

The transmission amplitude can be found from the equation $t = t_0 + \lim_{\xi\to+\infty}\frac{(1,0)\cdot\tilde{\chi}(\xi)}{u_L(-\xi)}$. Using Eq. (9b) we obtain for the correction $\delta\mathcal{T}$ to the transmission coefficient,

$$\frac{\delta\mathcal{T}}{\lambda} = -\frac{3e^{-\frac{\pi q^2}{2}}}{1+|\alpha|^2}\int d\xi' n(\xi')\mathrm{Im}[\alpha^*\psi_R^\dagger(\xi')\psi_L(\xi')]. \qquad (15)$$

It may be evaluated using Eqs. (7), (4), (5) and (11), and is plotted as a function of q in Fig. 2 b). At weak reflection, $q < 1$, the correction to transmission coefficient is small even if the interaction constant is of order unity. This is because the Friedel oscillations amplitude is proportional to the reflection amplitude. Thus the noninteracting result, Eq. (1), provides a good description for the low temperature conductance of metallic devices. In the tunneling regime, $q \gg 1$, the relative correction to the transmission amplitude is expected to be strong because of the exponential dependence of the tunneling amplitude on the effective electric field. Therefore the method described above becomes inapplicable.

In summary, the low temperature magnetoconductance of p-n junctions in clean single wall carbon nanotubes was studied in the geometry where the magnetic field is along the tube axis. For weak band-tilting field $E \ll \hbar v/eR^2$ the magnetoconductance of long, $L \gg R$, junctions becomes of order unity while the flux through the tube is much smaller than the flux quantum. In the noninteracting electron approximation the device conductance is given by Eq. (1). The magnetoconductance is positive for metallic tubes and nonmonotonic for semiconducting and small gap tubes. The interaction correction to the zero temperature magnetoconductance was studied to first order in perturbation theory. It arises due to the change in the effective electric field in the gap between the p- and n- regions and due to the scattering from the Friedel oscillations. In contrast to the one-dimensional Fermi gas, the Friedel oscillations in the present geometry fall off as $1/x^2$, which leads to the absence of infrared divergence in the correction to the tunneling amplitude. The net correction to the tunneling probability is positive. It is given by Eq. (15) and is plotted in Fig. 2 b). If the reflection coefficient is not too strong the noninteracting electron result, Eq. (1), is rather accurate even if the coupling constant is of order unity. At finite temperatures, in addition to tunneling across the classically forbidden region electrons can be transferred between p- and n- regions by being promoted across the band gap due to inelastic electron-electron and electron phonon scattering. The estimate of activation transfer rate shows that tunneling processes described by Eq. (1) dominate the transport for $T < eER$.

I would like to thank D. Cobden, E. Mishchenko, T. D. Son and B. Spivak and for useful discussions.

[1] R. Peierls, *Quantum theory of solids*, Clarendon Press, 1955.
[2] H. Ajiki and T. Ando, J. Phys. Soc. Jpn. **62**, 1255 (1993); ibid. **65**, 505 (1996).
[3] J. Cao *et al.*, Phys. Rev. Lett. **93**, 216803 (2004).
[4] Liang, W. *et al.*, Nature **411**, 665 (2001).
[5] Kong, J. *et al.*, Phys. Rev. Lett. **87**, 106801 (2001).
[6] E.L. Ivchenko and B. Spivak, Phys. Rev. B **66**, 155404 (2002).
[7] J. Wei *et al.*, Phys. Rev. Lett. **95** 256601 (2005).
[8] G. Fedorov *et al.*, Nano Lett. **7**, 960 (2007).
[9] H. T. Man, and A. F. Morpurgo, Phys. Rev. Lett. **95**, 026801 (2005).
[10] T. Dürkop, *et al.*, Nano Lett. **4**, 35 (2004).
[11] S. Ilani, *et al.*, Nature Physics **2**, 687 (2006).

[12] K.A. Matveev, D. Yue, and L.I. Glazman, Phys. Rev. Lett. **71**, 3351 (1993); D. Yue, L.I. Glazman, and K.A. Matveev, Phys. Rev. B **49**, 1966 (1994).
[13] V. V. Cheianov and V. I. Fal'ko, Phys. Rev. B **74**, 041403(R) (2006).
[14] P. M. Morse, and H. Feshbach, *Methods of theoretical physics*, McGraw-Hill (1953).